Research article

NMR IN BIOMEDICINE

Received: 19 November 2012, Revised: 24 May 2013, Accepted: 6 July 2013, Published online in Wiley Online Library

(wileyonlinelibrary.com) DOI: 10.1002/nbm.3008

# Interrelation of $^{31}$P-MRS metabolism measurements in resting and exercised quadriceps muscle of overweight-to-obese sedentary individuals

Ladislav Valkovič[a,b], Barbara Ukropcová[c,d], Marek Chmelík[a], Miroslav Baláž[c], Wolfgang Bogner[a], Albrecht Ingo Schmid[a,e], Ivan Frollo[b], Erika Zemková[f], Iwar Klimeš[c], Jozef Ukropec[c], Siegfried Trattnig[a] and Martin Kršňák[a,g]*

**Phosphorus magnetic resonance spectroscopy ($^{31}$P-MRS) enables the non-invasive evaluation of muscle metabolism. Resting Pi-to-ATP flux can be assessed through magnetization transfer (MT) techniques, and maximal oxidative flux ($Q_{max}$) can be calculated by monitoring of phosphocreatine (PCr) recovery after exercise. In this study, the muscle metabolism parameters of 13 overweight-to-obese sedentary individuals were measured with both MT and dynamic PCr recovery measurements, and the interrelation between these measurements was investigated. In the dynamic experiments, knee extensions were performed at a workload of 30% of maximal voluntary capacity, and the consecutive PCr recovery was measured in a quadriceps muscle with a time resolution of 2 s with non-localized $^{31}$P-MRS at 3 T. Resting skeletal muscle metabolism was assessed through MT measurements of the same muscle group at 7 T. Significant linear correlations between the $Q_{max}$ and the MT parameters $k_{ATP}$ ($r = 0.77$, $P = 0.002$) and $F_{ATP}$ ($r = 0.62$, $P = 0.023$) were found in the study population. This would imply that the MT technique can possibly be used as an alternative method to assess muscle metabolism when necessary (e.g. in individuals after stroke or in uncooperative patients).** **Copyright © 2013 John Wiley & Sons, Ltd.**

*Supporting information may be found in the online version of this paper*

**Keywords:** muscle metabolism; $^{31}$P-MRS; PCr recovery; magnetization transfer; obesity

## INTRODUCTION

Muscle energy metabolism that fuels muscle contractile activity is primarily regulated by the maximal ATP synthesis rate, which is controlled by the ATP/ADP ratio in the cytosol (1), and which is under aerobic conditions in sub-maximally exercised muscle, mainly determined by the oxidative phosphorylation capacity of mitochondria. As the majority of glucose uptake and glycogen storage in response to insulin occurs in skeletal muscle (2), the skeletal muscle is considered an important target of insulin

* *Correspondence to: Martin Kršňák, Division of Endocrinology and Metabolism, Department of Internal Medicine III, Medical University of Vienna. E-mail: martin.krssak@meduniwien.ac.at*

a *L. Valkovič, M. Chmelík, W. Bogner, A. I. Schmid, S. Trattnig, M. Kršňák MR Centre of Excellence, Department of Radiology, Medical University of Vienna, Vienna, Austria*

b *L. Valkovič, I. Frollo Department of Imaging Methods, Institute of Measurement Science, Slovak Academy of Sciences, Bratislava, Slovak Republic*

c *B. Ukropcová, M. Baláž, I. Klimeš, J. Ukropec Obesity Section, Diabetes and Metabolic Disease Laboratory, Institute of Experimental Endocrinology, Slovak Academy of Sciences, Bratislava, Slovak Republic*

d *B. Ukropcová Faculty of Medicine, Comenius University, Bratislava, Slovak Republic*

e *A. I. Schmid Centre for Medical Physics and Biomedical Engineering, Medical University of Vienna, Vienna, Austria*

f *E. Zemková Faculty of Physical Education and Sport, Comenius University, Bratislava, Slovak Republic*

g *M. Kršňák Division of Endocrinology and Metabolism, Department of Internal Medicine III, Medical University of Vienna, Vienna, Austria*

**Abbreviations used:** *$^{13}$C-MRS, carbon magnetic resonance spectroscopy; $^{31}$P-MRS, phosphorus magnetic resonance spectroscopy; BMI, body mass index; CK, creatine kinase; $\Delta PCr_{recovery}$, the amount of PCr replenished during the recovery period; $F_{CK}$, $F_{ATP}$, forward flux of the CK reaction and Pi-to-ATP reaction; HOMA-IR, homeostasis model of assessment – insulin resistance; IR, insulin resistance; $k_{CK}$, $k_{ATP}$, forward rate constants of the CK reaction and Pi-to-ATP reaction; LBM, lean body mass; MT, magnetization transfer; MVC, maximal voluntary contraction; $pH_i$, intracellular pH; $PCr_{end\_recovery}$, the amount of PCr at the end of the recovery period; $Q_{max}$, maximal oxidative flux; $T_1^{app}$, apparent longitudinal relaxation; T2D, type II diabetes; TCA, tricarboxylic acid; TI, inversion delay; $\tau_{PCr}$, time constant of the PCr recovery; $VO_{2max}$, maximal whole-body oxygen uptake capacity; $V_{PCr}$, initial PCr recovery rate; %FAT, the body/fat composition.*



Copyright © 2013 John Wiley & Sons, Ltd.

action. It has been recently shown that insulin resistance reflects not only defects in glucose uptake, but also abnormalities of the mitochondrial content, distribution, and function in the skeletal muscle (3–6). Changes related to these mitochondrial pathologies could indicate profound defects in lipid metabolism, resulting in the progression of obesity and metabolic disease even in a young, sedentary population (7,8).

Phosphorus magnetic resonance spectroscopy ($^{31}$P-MRS) enables the non-invasive measurement of intracellular phosphorus containing metabolites (i.e., phosphocreatine – PCr, ATP, and inorganic phosphate – Pi), and thus is the ideal tool for *in vivo* monitoring of the cell energy status and metabolism (1,9). Metabolite concentrations can be measured in the equilibrium state.

Dynamic $^{31}$P-MRS during exercise and consecutive recovery provides a technique for the determination of the rate of oxidative ATP synthesis in challenged muscle (10–12). The parameters of the PCr recovery experiment most likely reflect the maximal *in vivo* muscle mitochondrial output or capacity (1), because, in aerobic conditions, PCr is resynthesized almost exclusively through oxidative ATP synthesis (10). Several $^{31}$P-MRS studies have reported that a prolonged time for PCr recovery is associated with elevated fasting plasma glucose or insulin resistance (13,14).

The resting Pi-to-ATP flux ($F_{ATP}$) can be determined by a $^{31}$P-MRS magnetization transfer (MT) technique (15,16). Compared with young healthy volunteers, a decreased Pi-to-ATP exchange was reported, along with insulin resistance (IR), in the offspring of type 2 diabetes (T2D) patients (17) and in patients with overt T2D (15). In general, $F_{ATP}$ is considered to reflect the resting ATP demand (6,17,18), but, as the $F_{ATP}$ obtained by MT measurements consists of both mitochondrial (oxidative) ATP synthase flux and glycolytic ATP exchange flux (and, therefore, overestimates the skeletal muscle ATP synthesis rate at rest), lower $F_{ATP}$ values do not necessarily reflect a mitochondrial defect (19). However, even though the absolute values of metabolic fluxes differ between the results from MT experiments and other methods of oxidative metabolism observation (e.g. the tricarboxylic acid – TCA – cycle flux measurements via $^{13}$C-MRS), the relative differences found in the elderly and IR subjects compared with controls point in the same direction (17,20,21). Earlier, a linear correlation between the Pi-to-ATP flux, measured by MT, and the net ATP synthesis, measured by PCr depletion during cuff ischemia, was reported, suggesting that $F_{ATP}$ could be used as a surrogate marker for net ATP synthesis at rest (22).

Which of these two methods is more suitable for the measurement of *in vivo* mitochondrial function, and whether the parameters of oxidative metabolism calculated by these two techniques correlate, has been the topic of much discussion recently (22,23). These comparisons have been performed either in rats with mitochondrial dysfunction (23) or in lean, healthy volunteers (22), with different results.

The possibility of using MT experiments rather than the exercise–recovery experiments would be very attractive for the diagnosis of injured or diseased skeletal muscles, for treatment monitoring and/or for uncooperative patients. The aim of this study was, therefore, to compare the metabolic parameters obtained by these two techniques – the resting state ATP synthesis flux and the post-exercise PCr recovery – and assess their interrelation in young, sedentary, overweight-to-obese individuals, a segment of the population typically prone to diabetes.

## MATERIALS AND METHODS

### Study population

Thirteen overweight-to-obese, sedentary volunteers (eight males, five females; 35.3 ± 6.7 yrs; range 22–46 yrs) participated in the study. Written, informed consent was obtained from all volunteers and the local ethics committee approved the protocol. The study inclusion criteria were BMI equal to or above 27.0 kg m$^{-2}$, sedentary lifestyle without regular physical activity, and no pharmacotherapy.

### Experimental design

Within a week before the MR examinations, all participants underwent a physical examination and physiological testing. BMI was measured by an analog weight scale and standard measuring tape. The body/fat composition (%Fat) and lean body mass (LBM) were estimated by the bioelectric impedance, as measured with an Omron BF511 (Omron Healthcare, Matsusaka, Japan). An estimate of insulin sensitivity and level of glucose intolerance were calculated from fasting levels of serum glucose and insulin (homeostatic model assessment of IR – HOMA-IR), and from the two-hour glucose level and from the area under the glycemic curve during an oral glucose tolerance test, respectively. Maximal aerobic capacity – whole-body oxygen uptake ($VO_{2max}$) – was measured on a Lode Corival cycle ergometer during an incremental exercise test until the point of submaximal workload (Lode, Groningen, The Netherlands). The gas exchange rate was measured continuously with the Ergostik (Geratherm Respiratory, Bad Kissingen, Germany). Maximal oxygen consumption rate was expressed relative to LBM. The time interval between ergometry and MR measurement was at least three days.

The maximal voluntary contraction of the whole leg was measured with the aid of a computer-controlled dynamometer, developed by the adaptation of a horizontal leg-press (FPES CU, Bratislava, Slovakia). The sedentary lifestyle was evaluated based on 14 days of accelerometer recordings and expressed as the number of steps per 24 hours. These values might differ between working days and weekends, thus both parameters were evaluated.

### MR measurements

All volunteers were tested in the morning two hours after a standardized breakfast. Both methods were tested on the same day. $^{31}$P-MRS exercise recovery examinations were performed on a 3 T scanner (TIM TRIO, Siemens Healthcare, Erlangen, Germany). $^{31}$P-MRS MT examinations were performed at a 7 T scanner (Magnetom, Siemens Healthcare, Erlangen, Germany) to gain SNR and achieve a significant reduction in measurement time while providing results similar to those obtained at 3 T, as has been demonstrated recently (24). Very similar dual-tuned ($^{31}$P/$^{1}$H) loop coils (10 cm diameter, Rapid Biomedical, Rimpar, Germany) were used on both systems and coil positions were marked for exact re-positioning in the other MR system. The sensitivity of the $^{31}$P channels of both coils was measured and it was confirmed that the same volume of interest would be measured at both field strengths (Fig 1). The volume of interest covered four of the quadriceps muscles that are actively involved in a knee extension exercise (25). As has been recently shown, the order of exercise–recovery and MT measurements does not influence the results (22), and experiments were performed in


Copyright © 2013 John Wiley & Sons, Ltd.

NMR IN BIOMEDICINE

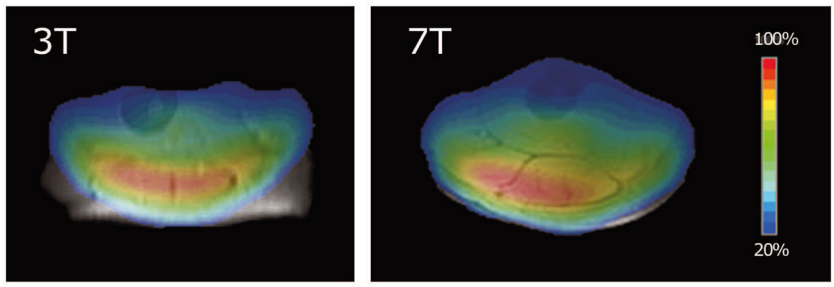


**Figure 1**. Sensitivity maps of the $^{31}$P channels of both surface coils overlaid on the quadriceps images of the same volunteer show that the same muscle groups (all involved in the performed exercise) are measured on both MR systems.

a pseudo-random order of the MR methods to measure two volunteers simultaneously and save experiment time.

### Rest–exercise–recovery experiment

The subjects were lying in a prone position fixed to the ergometer for knee extensions (Ergospect, Innsbruck, Austria) with the left quadriceps femoris muscle positioned over the surface coil. Magnetic field homogeneity was optimized by monitoring the water resonance with the lower leg positioned in the exercise position. For the assessment of metabolite concentrations, a partially relaxed spectrum ($T_R$ 15 s, 16 scans) was recorded at rest and corrections were performed for the longitudinal relaxation times, as measured by Bogner *et al*. (26). The γ-ATP resonance was used rather than the β-ATP as an internal reference, because the shape of the excitation pulse did not guarantee a reliable excitation of β-ATP. A standardized exercise protocol was performed according to Layec *et al*. (27). After a 2 min resting period, the subjects performed a dynamic exercise for 6 min followed by a 6 min recovery period. Exercise consisted of knee extensions against a calculated air pressure at 0.5 Hz. Contraction–relaxation periods were gated to the data acquisition on the basis of an audio signal, so that spectra were always recorded in a relaxed state of the muscle. The workload was set to 30% of the maximal voluntary contraction (MVC) of the left leg, based on previous leg-press and calibration examinations.

A pulse–acquire sequence was used ($T_R$ 2 s; 400 μs block pulse excitation; 42° flip angle adjusted to give maximal SNR/unit of time; bandwidth 3 kHz; vector size 1024) for data acquisition and every scan was saved separately, thus enabling a temporal resolution of 2 s.

### Magnetization transfer experiment

Resting-state ATP turnover was measured using an MT experiment, as described in (16) and as subsequently optimized (24). The subjects were lying in a supine position with the surface coil fixed over the left quadriceps femoris muscle. Baseline intramyocellular concentrations of phosphorus metabolites were assessed based on $T_1$-corrected, partially relaxed baseline spectra ($T_R$ 15 s, 16 averages), as described above. The exchange between γ-ATP and PCr (i.e., CK reaction) and between γ-ATP and Pi (i.e., ATP-synthesis) was investigated (16,20). The MT protocol consisted of 24 non-localized spectrum acquisitions: during continuous frequency-selective, γ-ATP saturation at −2.48 ppm (steady state; eight averages); during continuous saturation at a downfield frequency mirrored around PCr at 2.48 ppm (equilibrium PCr state; eight averages); and during continuous saturation at a downfield frequency equidistant to Pi at 12.52 ppm (equilibrium Pi state, eight averages). The apparent longitudinal relaxation times of PCr ($T_1^{app}{}_{PCr}$) and Pi ($T_1^{app}{}_{Pi}$) were determined by performing an inversion recovery experiment ($\tau$–180°–inversion delay ($T_I$)–90°–acquire) during selective saturation of the γ-ATP resonance (eight $T_I$ values = 100, 300, 500, 700, 1500, 3000, 5000, 8000 ms; two averages). A pulse–acquire sequence ($T_R$ 15 s, block pulse 400 μs excitation) was used for MT experiments, with a total measurement time of 14 min 36 s.

### Data analysis

All measured spectra were analyzed using jMRUI (version 4.0) with the AMARES algorithm (28). PCr and Pi peaks were fit as single Lorentzians, whereas γ- and α-ATP signals were fitted as Lorentzian doublets and β-ATP as a triplet. Line widths of Pi and γ-ATP were constrained with respect to the line width of the PCr peak. For the absolute quantification of metabolite concentrations, an ATP concentration of 8.2 mM cellular water was assumed (29). The chemical shift of Pi relative to PCr in parts per million ($\delta$) was used to calculate the intracellular pH ($pH_i$) (30), according to the Henderson–Hasselbalch equation.

To fit the spectra obtained during the saturation inversion recovery experiment, the line widths of PCr and Pi were determined from the last inversion recovery scan (i.e. with $T_I$ = 8000 ms). This provides sufficient stability to fit inversion recovery spectra with peaks of different $T_I$ values using the AMARES algorithm. The amplitudes obtained from the steady-state measurement with selective suppression of γ-ATP (−2.48 ppm) were also incorporated into the $T_1^{app}$ calculation.

### PCr recovery kinetics

During the recovery period, PCr signal time changes were fitted to a mono-exponential function, providing the time constant of the PCr recovery rate ($\tau_{PCr}$). This was used to calculate the initial PCr recovery rate ($V_{PCr}$), which roughly represents ATP turnover at the end of exercise. The maximal rate of oxidative phosphorylation ($Q_{max}$) was calculated according to the ADP-based model of Michaelis and Menten.

### Resting state turnover fluxes

The $T_1^{app}$ values of PCr and Pi were determined by fitting the inversion recovery data with a monoexponential function with three degrees of freedom to account for the possibility of partial saturation (26), using Matlab (MathWorks, Natick, MA, USA). The forward rate constants for the CK reaction and Pi-to-ATP reaction ($k_{CK}$ and $k_{ATP}$, respectively) were calculated from the fractional


Copyright © 2013 John Wiley & Sons, Ltd.

reduction of PCr and Pi magnetization upon selective saturation of γ-ATP. The resting forward exchange fluxes ($F_{CK}$, $F_{ATP}$) were also calculated.

For a more detailed description of the metabolic parameter calculation from $^{31}$P MRS data, see the supplementary material.

### Statistical analysis

The statistical analyses were performed using SPSS for Windows software (SPSS, Chicago, IL, USA).

The relationships between physiological characteristics and the $^{31}$P-MRS parameters, and between the variables of the MT experiment and the exercise–recovery experiment, were analyzed using linear regressions. Linear regression was used because the background relation is still unclear and previous study showed linear correlation (22). The corresponding strengths were assessed using Pearson's correlation coefficient. Results are presented as average ± SEM and were considered statistically significant at $p < 0.05$.

As it is known that $\tau_{PCr}$ largely depends on the end-exercise $pH_i$ (31), and this is linked to the relative amount of the PCr drop at the end of exercise (32), the correlations between $\tau_{PCr}$ and the parameters derived from the MT experiment were assessed for the whole study population and also for two subgroups, based on the exercise-induced PCr drop, with the cut-off set at 40%, as determined by a post hoc analysis. The comparison between the subgroups was performed with an unpaired *t*-test, and results were considered significant at $p < 0.05$.

**Table 1.** Characteristics of the studied population.

| Gender | 8m/5f |
|---|---|
| Age [yrs] | 35.3 ± 6.7 |
| BMI [kg m$^{-2}$] | 30.79 ± 2.25 |
| Body fat [%] | 34.4 ± 1.9 |
| LBM [kg] | 62.80 ± 11.68 |
| HOMA IR | 1.67 ± 0.27 |
| $VO_{2max}$/LBM [ml min$^{-1}$ kg$^{-1}$] | 34.1 ± 2.1 |
| Maximal voluntary contraction [N]# | 2401 ± 198 |
| Steps per 24 hours working day* | 7223 ± 624 |
| Steps per 24 hours weekend* | 5886 ± 370 |

#as determined by the leg-press dynamometer.
*14 days of accelerometer recordings were used for analysis.

## RESULTS

### Study participants

Average BMI was 30.8 ± 2.3 kg m$^{-2}$ (range 27.2–35.0 kg m$^{-2}$) and maximal aerobic capacity ($VO_{2max}$) averaged to 34.1 ± 2.1 ml min$^{-1}$ per kg of LBM (range 18.6–40.6 ml min$^{-1}$ per kg of LBM). Detailed characteristics of the subjects are presented in Table 1.

### PCr recovery after exercise

Dynamic $^{31}$P-MRS measurements of the quadriceps muscle during knee-extension exercise and subsequent recovery were performed. PCr concentration decreased rapidly by a mean of 12.6 ± 7.3 mM during exercise, and increased rapidly to the starting value, following a roughly monoexponential curve, after the end of exercise. The values of metabolite concentrations (PCr, Pi, ADP) and the pH calculated at rest and at the end of exercise are given in Table 2. The time evolution of PCr concentration during the exercise–recovery experiment and a monoexponential fit of the recovery phase are depicted in Figure 2. The values of the initial PCr recovery rate ($V_{PCr}$), the PCr recovery time constant ($\tau_{PCr}$), and the maximal oxidative flux ($Q_{max}$) are also given in Table 2.

### Magnetization transfer

Figure 3 shows an example of a typical $^{31}$P MT spectrum measured in the resting quadriceps muscle, with frequency-selective saturation of the γ-ATP peak and corresponding reference spectra with saturation at a downfield frequency mirrored around PCr and around Pi. The values of measured $T_1^{app}$, $k_{CK}$, $k_{ATP}$, $F_{CK}$, and $F_{ATP}$ are given in Table 2.

### Subgroup analysis

The study population was divided according to the exercise-induced PCr drop, with the cut-off set at 40%, yielding seven participants with the smaller PCr drop (group S; $n = 7$) and six participants with the larger PCr drop (group L; $n = 6$). The subgroups showed significant differences in the PCr drop (S 24.9% ± 8.0% versus L 59.2% ± 13.2%, $p = 0.0001$), end-exercise $pH_i$ (S 7.05 ± 0.01 versus L 6.99 ± 0.06, $p = 0.008$), $\tau_{PCr}$ (S 30.0 s ± 6.5 versus L 48.4 s ± 6.3, $p = 0.0003$), and $V_{PCr}$ (S 0.23 mM s$^{-1}$ ± 0.05 versus L 0.39 mM s$^{-1}$ ± 0.08, $p = 0.001$). There was no overlap in the end-exercise $pH_i$ values between the two subgroups. There were no significant differences in measured physical characteristics

**Table 2.** Results of the magnetization transfer and rest–exercise–recovery experiments.

| | | Exercise–recovery experiment | | | MT experiment | |
|---|---|---|---|---|---|---|
| | Baseline | End of exercise | PCr recovery | | | |
| PCr [mM] | 32.2 ± 6.1 | 19.6 ± 7.6 | PCr drop [%] | 40.7 ± 20.5 | $T_{1\,PCr}^{app}$ [s] | 1.8 ± 0.2 |
| Pi [mM] | 4.1 ± 0.7 | 10.7 ± 3.0 | $\tau_{PCr}$ [s] | 38.5 ± 11.3 | $T_{1\,Pi}^{app}$ [s] | 4.0 ± 0.6 |
| Pi/PCr | 0.13 ± 0.02 | 0.63 ± 0.28 | $V_{PCr}$ [mM s$^{-1}$] | 0.31 ± 0.11 | $k_{CK}$ [s$^{-1}$] | 0.26 ± 0.05 |
| ADP [μM] | 10.4 ± 0.5 | 69.4 ± 63.5 | $Q_{max}$ [mM s$^{-1}$] | 0.49 ± 0.08 | $k_{ATP}$ [s$^{-1}$] | 0.07 ± 0.02 |
| $pH_i$ | 7.08 ± 0.02 | 7.03 ± 0.05 | | | $F_{CK}$ [mM s$^{-1}$] | 9.36 ± 2.60 |
| | | | | | $F_{ATP}$ [mM s$^{-1}$] | 0.25 ± 0.07 |


Copyright © 2013 John Wiley & Sons, Ltd.

NMR IN BIOMEDICINE

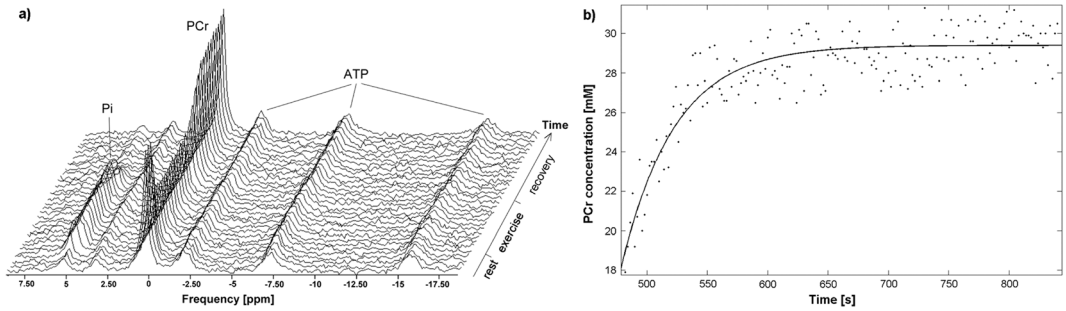


**Figure 2**. (a) Time course of the $^{31}$P spectra during rest, exercise, and subsequent recovery. For better reading, only a few representative spectra were chosen for graphic presentation. (b) Time course of the PCr concentration during the recovery phase. The solid line indicates the exponential fit for the estimation of $\tau_{PCr}$.

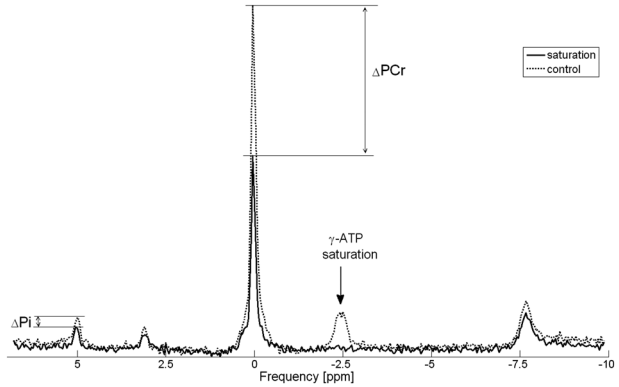


**Figure 3**. $^{31}$P spectra showing the magnetization transfer effect on PCr and Pi. Arrows indicate the saturation frequency at γ-ATP in the saturation experiment (solid line) and the saturation effects on the chemical exchange partners (PCr and Pi) compared with the control experiment (dotted line). Note that the control experiment consists of two separate measurements, which were, for display purposes only, combined (the connection point is 2.5 ppm).

or in the resting metabolism parameters, as defined by the MT experiments between the defined subgroups.

### Correlation analysis

There was no significant correlation found between the physiological parameters (age, BMI, %Fat, LBM) and the parameters of both $^{31}$P-MRS methods ($\tau_{PCr}$, $V_{PCr}$, $Q_{max}$, $k_{CK}$, $F_{CK}$, $k_{ATP}$, $F_{ATP}$).

The maximal oxidative flux measured by exercise recovery was significantly correlated with MT parameters (representative correlations are depicted in Fig. 4). $Q_{max}$ linearly correlated with

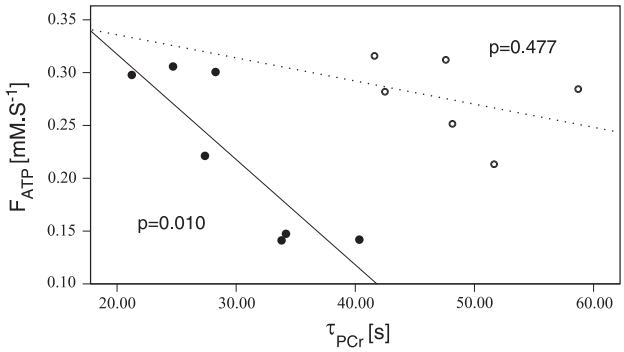


**Figure 5**. Plot showing the correlation between the PCr recovery constant ($\tau_{PCr}$) and $F_{ATP}$. The filled symbols and the solid line depict the subgroup with the smaller PCr (S) decline and its linear correlation, and the open symbols and the dashed line depict the subgroup with the larger PCr (L) decline and corresponding correlation.

$k_{CK}$ ($r = 0.66$, $P = 0.014$), and $F_{CK}$ ($r = 0.61$, $P = 0.027$), and also with $k_{ATP}$ ($r = 0.80$, $P = 0.001$) and $F_{ATP}$ ($r = 0.66$, $P = 0.014$).

There was no significant relationship between $\tau_{PCr}$ and any of the MT parameters in the entire population. However, when divided into subgroups based on the exercise-induced PCr drop, a significant correlation was found between $\tau_{PCr}$ and $k_{ATP}$ ($r = -0.81$, $P = 0.027$) and between $\tau_{PCr}$ and $F_{ATP}$ ($r = -0.87$, $P = 0.010$) in the subgroup with the smaller PCr drop (S). However, there was no correlation in the subgroup with the larger PCr decline (L) (Fig. 5). Correlation analysis yielded similar results when the relation between the inverse value of $\tau_{PCr}$, the rate constant of PCr recovery, and the MT parameters was investigated.

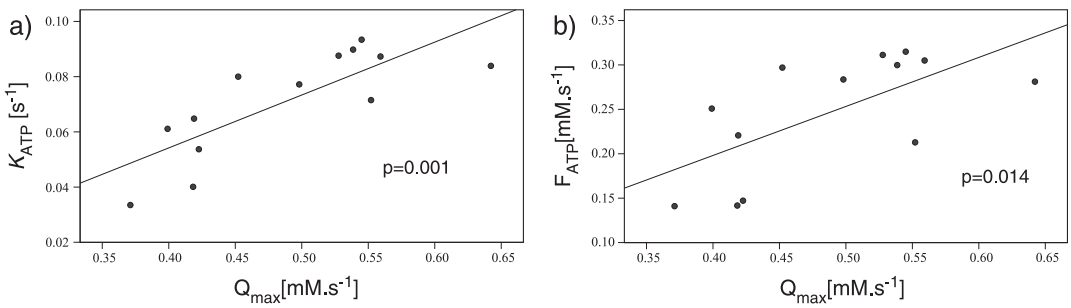


**Figure 4**. Plots showing the correlations of maximal oxidative flux ($Q_{max}$) with $k_{ATP}$ (a) and $F_{ATP}$ (b).


Copyright © 2013 John Wiley & Sons, Ltd.

## DISCUSSION

In this study, we compared two $^{31}$P-MRS methods for energy metabolism examination *in vivo* – the post-exercise PCr recovery and magnetization transfer (MT) – in the quadriceps muscles of young, overweight-to-obese, sedentary, non-diabetic subjects. We were able to show a significant correlation between the resting ATP synthesis flux, measured by MT, and the maximal oxidative flux, measured by PCr post-exercise recovery. To the best of our knowledge, no direct comparison of MT and exercise–recovery experiments has been reported in this type of population and muscle group.

Mitochondrial capacity has been previously shown to be impaired based on training status, resulting in decreased $Q_{max}$ and longer $\tau_{PCr}$ in sedentary populations (33,34); similar trends were found in the current study. The comparison of our results with previously published data on quadriceps exercise of obese and/or sedentary subjects (33–36) is summarized in Table 3. In detail, the values of $V_{PCr}$ and $Q_{max}$ obtained in our study are in good agreement with previously published results from the quadriceps muscle (35). The time constant of the PCr recovery, $\tau_{PCr}$, of 38 ± 11 s measured in the overweight-to-obese, prone-to-diabetes subjects reported here tended to be shorter than those reported in previously published PCr recovery studies of healthy, lean sedentary subjects (35), and also of healthy, obese sedentary subjects (36). In healthy, lean subjects (35) $\tau_{PCr}$ was reported to be 53 ± 25 s, and in healthy obese subjects (36) 44 ± 10 s; thus, this measure seems to be independent of the obesity phenotype, and instead reflects muscle fitness. However, as several previous reports have clearly shown, PCr recovery is significantly slower in the presence of intracellular acidosis (31,37,38); thus, our shorter recovery constant could also be explained by the absence of acidosis at the end of exercise in our study ($pH_i$ = 7.03 ± 0.05), compared with the end of exercise conditions in the other aforementioned studies ($pH_i$ = 6.80 ± 0.23 in (35), $pH_i$ = 6.91 ± 0.08 in (36)). Individual differences caused by different subject pools, particularly the age of subjects and also the gender-related heterogeneity of our study population (five females/eight males), should also be considered. Importantly, $Q_{max}$ has been shown to be independent of $pH_i$ unless a severe acidosis is observed ($pH < 6.5$) (37,39–41), so it seems to be a more appropriate parameter for the assessment of mitochondrial function.

The values of CK and Pi-to-ATP fluxes reported in our study accord well with other MT studies performed in human skeletal muscle (22,42–44). The slightly longer apparent relaxation times reported in this study, compared with previously reported data from calf muscle at 7 T (24), might be attributable to the differences in the analyzed muscle group and the phenotypic characteristics of the study population.

We report a significant correlation between $Q_{max}$, measured by an exercise–recovery experiment, and forward rate fluxes, measured by MT at rest ($F_{ATP}$, $F_{CK}$), in young, sedentary overweight-to-obese individuals. This finding is in good agreement with a recent human calf muscle study of lean volunteers, which showed a significant correlation between $F_{ATP}$ and $Q_{max}$ (22). Even though the data obtained by Schmid *et al.* (22) were measured in the calf muscle of healthy lean subjects under partially ischemic conditions, pooled analysis of their and our results showed significantly positive linear correlation ($r$ = 0.474, $p$ = 0.011; Fig. 6). Slight differences in mean $V_{PCr}$ and $Q_{max}$ values could be attributed to the different muscles investigated or the sedentary nature of volunteers examined in our study. Based on the results of the aforementioned study, it was reasonable to investigate whether the Pi-to-ATP flux rate, as measured by MT, would correlate with $Q_{max}$ measured by PCr recovery in the quadriceps muscle of sedentary overweight-to-obese individuals. The mechanisms underlying this observed relation still remain unclear. We also report a significant correlation between the $Q_{max}$ and the forward rate constants of the chemical exchange reactions ($k_{ATP}$, $k_{CK}$). The resting concentration of Pi did not significantly correlate with $Q_{max}$, possibly signaling a

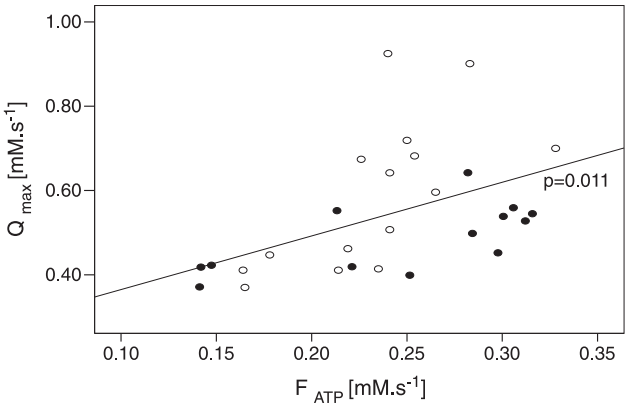


**Figure 6**. Plot showing the results of a pooled analysis of the current results (filled symbols) and the results from the published study by Schmid *et al.* (22) (open symbols). Note that, even though the data of Schmid *et al.* were measured in the calf muscle of healthy lean subjects under partially ischemic conditions, significantly positive linear correlation of $F_{ATP}$ and $Q_{max}$ was found ($p$ = 0.011).

**Table 3.** Comparison of current results with previous reports on quadriceps exercise in healthy obese and/or sedentary subjects.

| Study | Age of volunteers | BMI [kg m$^{-2}$] | $VO_{2max}$ [ml min$^{-1}$ kg$^{-1}$] | $pH_i$_end exercise | $\tau_{PCr}$ [s] | $Q_{max}$ [mM s$^{-1}$] |
|---|---|---|---|---|---|---|
| Layec *et al.* (33,35) | 35.0 ± 6 | 22.3 ± 5.1 | 42.3 ± 6.2* | 6.80 ± 0.23 | 53 ± 25 | 0.43 ± 0.06 |
| Johansen *et al.* (34) | 26.7 ± 1 | 19.6 ± 1.2 | — | 6.95 ± 0.06# | 53 ± 6 | 0.47 ± 0.10$ |
| De Feyter *et al.* (36) | 56.5 ± 6 | 32.9 ± 4.6 | 45.6 ± 6.0 | 6.91 ± 0.08 | 45 ± 11 | 0.69 ± 0.12 |
| Current study | 35.3 ± 7 | 30.8 ± 2.3 | 34.1 ± 2.1 | 7.03 ± 0.05 | 39 ± 11 | 0.49 ± 0.08 |

*Not stated if the $VO_{2max}$ value reported is calculated as a ratio to body weight or LBM.
#The pH value was taken only from a provided plot, so might not be perfectly accurate.
$The $Q_{max}$ value was recalculated for ATP concentration in the muscle of 8.2 mM.


Copyright © 2013 John Wiley & Sons, Ltd.

direct relationship between $Q_{max}$ and the Pi-to-ATP chemical exchange rate. PCr concentration, on the other hand, correlates with $Q_{max}$ significantly, and thus influences the relation between $Q_{max}$ and $F_{CK}$.

The study by Schmid *et al.* (22) also showed a correlation between $F_{ATP}$ and $\tau_{PCr}$, but, in our study, no correlation was found between $F_{ATP}$ and $\tau_{PCr}$ when the entire population was tested. Only when divided into two groups according to the level of PCr decline, with the cut-off set to 40%, did we observe a correlation in the subgroup with the smaller decline (S), characterized by a higher end-exercise $pH_i$ value as well, with no $pH_i$ overlap between the groups. No correlation between the rate constant of PCr recovery and $F_{ATP}$ has also been reported in an animal study using complex I blockers of the respiratory chain (23). Therefore, as discussed here and suggested in another publication (38), using $\tau_{PCr}$ as a direct measure of the mitochondrial capacity might be inappropriate if the end-exercise $pH_i$ varies across or differs between the study groups. In addition to the significant differences in PCr drop and end-exercise $pH_i$, our subgroups also differed significantly in the $\tau_{PCr}$ and $V_{PCr}$, but not in the $Q_{max}$ measurements, which again proves the $Q_{max}$ to be a more robust and appropriate parameter for characterizing the mitochondrial capacity.

Recently, it has been shown that the non-localized acquisition of mixed $^{31}$P spectra from exercising and relaxed muscle groups, as is the case with calf muscle exercise, significantly influences the results (45). In the case of the knee extension exercise, all four quadriceps muscles within the sensitive volume of the coil used in this study were active during the exercise (25). Therefore, in our study, the non-exercising muscle group is very unlikely to have influenced the results.

With regard to the MT measurement, one should keep in mind that this measurement determines fluxes in one direction; therefore, if the turnover reactions operate close to equilibrium, the measured unidirectional flux can be much higher than the net ATP flux (19,46). Furthermore, MT measures the ATP synthesis from all sources, including glycolysis, which has been shown to contribute significantly to $F_{ATP}$ measured by MT in yeast (47) and also in perfused rat hearts (48). Although the glycolysis is assumed to operate at very low rates in human skeletal muscle at rest (49), the coupled reaction, catalyzed by glycolytic enzymes, works near equilibrium, and the exchange between Pi and ATP may greatly exceed the net glycolytic flux (50). Thus, the absolute values of the ATP synthesis flux, as measured by the MT technique, are overestimated compared with other modalities used to study oxidative muscle metabolism (e.g. TCA cycle). Nevertheless, similar inter-group results for MT and TCA cycle parameters have been previously reported (20,21), suggesting that the $F_{ATP}$ metabolic flux responds to perturbations in mitochondrial metabolism (18).

As to the technical limitations of our study, we should note that the workload calibration method was not optimal. The leg-press exercise, used to assess the maximum voluntary contraction power of the lower limbs, activates a different spectrum of muscle groups than simple knee extension does, resulting in greater variations in the PCr drop, as expected. This was the reason we split the study subjects into two subgroups for the analysis of $\tau_{PCr}$ correlations. Nevertheless, the end-exercise $pH_i$ remained neutral and no significant acidification could be reported. The use of two different MR systems required subject repositioning, and, even though marks were provided and good care was taken to secure the same measurement position, some small mislocalization could not be fully excluded. Another issue is connected with the MR experiment itself. The radio-frequency bandwidth of the excitation pulse in the MT experiment is limited, considering the large frequency range of $^{31}$P resonances at 7 T. This might have affected the accurate quantification of distant off-resonant metabolites (β-ATP). Therefore, γ-ATP was used for concentration calculations as another accurate representative. The use of γ-ATP rather than β-ATP might slightly overestimate (<1%) the resting concentration of PCr and Pi. Application of alternative mathematical models for the analysis of the correlation between $Q_{max}$ and $F_{ATP}$ could possibly represent the correlation better. For better comparison with the previous studies and given the exploratory nature of our experiment, we opted for linear correlation only.

## CONCLUSION

Data collected in our study show that mitochondrial capacity, as determined by the maximal oxidative flux from PCr recovery kinetics ($Q_{max}$), correlates with the resting Pi-to-ATP flux, as well as with the CK resting state flux in overweight-to-obese sedentary subjects. This would suggest that an MT technique could provide a marker of skeletal muscle metabolism that correlates well with the exercise–recovery experiments. We also showed that the time constant of the PCr recovery ($\tau_{PCr}$) correlates with the MT values in a defined population only if the requirement for very low variability in end-exercise $pH_i$ is fulfilled.

## Acknowledgements

We thank all of the participants for their efforts and patience during data collection, Dr Radek Černý (MR Diagnostics, Czech Republic) for providing the instrumentation necessary for indirect calorimetry, Michal Jeleň and Martin Tkačov for their efforts in the calibration examinations of the maximum voluntary capacity, and Professor Dušan Hamar for kindly enabling us to use the leg-press dynamometer in our study. Our thanks are also extended to Dr Ivan Jelok for the comprehensive testing of the study participants with bicycle ergometry.

Parts of this study were presented at the ISMRM, 2012, Melbourne (Valkovic L *et al.* Skeletal muscle metabolism measured at rest and after exercise in obese non-diabetic subjects (poster ID 1436)).

This study was supported by the Vienna Spots of Excellence des Wiener Wissenschafts- und Technologie-Fonds (WWTF)–Vienna Advanced Imaging Center (VIACLIC to S. T.), by funds of the Oesterreichische Nationalbank (Anniversary Fund, project number: 15455 to L.V. and 13629 to M.C.), and by EFSD and a Lilly research fellowship (to B. U.), as well as by grants from the Agency of the Slovak Academy of Sciences, VEGA 2/0090/11, VEGA2/0174/12, and VEGA2/0198/11 (to I. F., B. U., and J. U.).

All authors and authors' institutions have no conflicts of interest to disclose.

## REFERENCES

1. Kemp GJ, Radda GK. Quantitative interpretation of bioenergetic data from 31P and 1H magnetic-resonance spectroscopic studies of skeletal-muscle – an analytical review. Magn. Reson. Q. 1994; 10(1): 43–63.
2. Defronzo RA, Bonadonna RC, Ferrannini E. Pathogenesis of NIDDM – a balanced overview. Diabetes Care 1992; 15(3): 318–368.

 Copyright © 2013 John Wiley & Sons, Ltd. 

3. Kelley DE, He J, Menshikova EV, Ritov VB. Dysfunction of mitochondria in human skeletal muscle in type 2 diabetes. Diabetes 2002; 51(10): 2944–2950.
4. Little JP, Gillen JB, Percival ME, Safdar A, Tarnopolsky MA, Punthakee Z, Jung ME, Gibala MJ. Low-volume high-intensity interval training reduces hyperglycemia and increases muscle mitochondrial capacity in patients with type 2 diabetes. J. Appl. Physiol.. 2011; 111(6): 1554–1560.
5. Rabol R, Boushel R, Dela F. Mitochondrial oxidative function and type 2 diabetes. Appl. Physiol. Nutr. Metab.–Physiol. Appl. Nutr. Metab. 2006; 31(6): 675–683.
6. Szendroedi J, Roden M. Mitochondrial fitness and insulin sensitivity in humans. Diabetologia 2008; 51(12): 2155–2167.
7. Morino K, Petersen KF, Shulman GI. Molecular mechanisms of insulin resistance in humans and their potential links with mitochondrial dysfunction. Diabetes 2006; 55: S9–S15.
8. Ukropec J, Ukropcova B, Kurdiova T, Gasperikova D, Klimes I. Adipose tissue and skeletal muscle plasticity modulates metabolic health. Arch. Physiol. Biochem. 2008; 114(5): 357–368.
9. Kemp GJ, Meyerspeer M, Moser E. Absolute quantification of phosphorus metabolite concentrations in human muscle in vivo by P-31 MRS: a quantitative review. NMR Biomed.. 2007; 20(6): 555–565.
10. Quistorff B, Johansen L, Sahlin K. Absence of phosphocreatine resynthesis in human calf muscle during ischemic recovery. Biochem. J. 1993; 291: 681–686.
11. Petersen SR, Gaul CA, Stanton MM, Hanstock CC. Skeletal muscle metabolism during short-term, high-intensity exercise in prepubertal and pubertal girls. J. Appl. Physiol.. 1999; 87(6): 2151–2156.
12. Tonson A, Ratel S, Le Fur Y, Vilmen C, Cozzone PJ, Bendahan D. Muscle energetics changes throughout maturation: a quantitative (31)P-MRS analysis. J. Appl. Physiol.. 2010; 109(6): 1769–1778.
13. Scheuermann-Freestone M, Madsen PL, Manners D, Blamire AM, Buckingham RE, Styles P, Radda GK, Neubauer S, Clarke K. Abnormal cardiac and skeletal muscle energy metabolism in patients with type 2 diabetes. Circulation 2003; 107(24): 3040–3046.
14. Schrauwen-Hinderling VB, Kooi ME, Hesselink MKC, Jeneson JAL, Backes WH, van Echteld CJA, van Engelshoven JMA, Mensink M, Schrauwen P. Impaired in vivo mitochondrial function but similar intramyocellular lipid content in patients with type 2 diabetes mellitus and BMI-matched control subjects. Diabetologia 2007; 50(1): 113–120.
15. Szendroedi J, Schmid AI, Chmelik M, Toth C, Brehm A, Krssak M, Nowotny P, Wolzt M, Waldhaus W, Roden M. Muscle mitochondrial ATP synthesis and glucose transport/phosphorylation in type 2 diabetes. PLoS Med.. 2007; 4(5): 858–867.
16. Brindle KM, Blackledge MJ, Challiss RA, Radda GK. 31P NMR magnetization-transfer measurements of ATP turnover during steady-state isometric muscle contraction in the rat hind limb in vivo. Biochemistry 1989; 28(11): 4887–4893.
17. Petersen KF, Dufour S, Befroy D, Garcia R, Shulman GI. Impaired mitochondrial activity in the insulin-resistant offspring of patients with type 2 diabetes. New Engl. J. Med. 2004; 350(7): 664–671.
18. Befroy DE, Rothman DL, Petersen KF, Shulman GI. $^{31}$P-magnetization transfer magnetic resonance spectroscopy measurements of in vivo metabolism. Diabetes 2012; 61(11): 2669–2678.
19. Kemp GJ, Brindle KM. What do magnetic resonance-based measurements of Pi → ATP flux tell us about skeletal muscle metabolism? Diabetes 2012; 61(8): 1927–1934.
20. Lebon V, Dufour S, Petersen KF, Ren J, Jucker BM, Slezak LA, Cline GW, Rothman DL, Shulman GI. Effect of triiodothyronine on mitochondrial energy coupling in human skeletal muscle. J. Clin. Invest.. 2001; 108(5): 733–737.
21. Petersen KF, Befroy D, Dufour S, Dziura J, Ariyan C, Rothman DL, DiPietro L, Cline GW, Shulman GI. Mitochondrial dysfunction in the elderly: possible role in insulin resistance. Science 2003; 300(5622): 1140–1142.
22. Schmid AI, Schrauwen-Hinderling VB, Andreas M, Wolzt M, Moser E, Roden M. Comparison of measuring energy metabolism by different $^{31}$P-magnetic resonance spectroscopy techniques in resting, ischemic, and exercising muscle. Magn. Reson. Med. 2012; 67(4): 898–905.
23. van den Broek NMA, Ciapaite J, Nicolay K, Prompers JJ. Comparison of in vivo postexercise phosphocreatine recovery and resting ATP synthesis flux for the assessment of skeletal muscle mitochondrial function. Am. J. Physiol. Cell Physiol. 2010; 299(5): C1136–U325.
24. Valkovič L, Chmelik M, Just Kukurová I, Krššák M, Gruber S, Frollo I, Trattnig S, Bogner W. Time-resolved phosphorus magnetization transfer of the human calf muscle at 3T and 7T: a feasibility study. Eur. J. Radiol.. 2013; 82(5): 745–751.
25. Richardson RS, Frank LR, Haseler LJ. Dynamic knee-extensor and cycle exercise: functional MRI of muscular activity. Int. J. Sports Med. 1998; 19(3): 182–187. DOI: 10.1055/s-2007-971901.
26. Bogner W, Chmelik M, Schmid AI, Moser E, Trattnig S, Gruber S. Assessment of (31)P relaxation times in the human calf muscle: a comparison between 3 T and 7 T in vivo. Magn. Reson. Med. 2009; 62(3): 574–582.
27. Layec G, Bringard A, Vilmen C, Micallef JP, Le Fur Y, Perrey S, Cozzone PJ, Bendahan D. Accurate work-rate measurements during in vivo MRS studies of exercising human quadriceps. Magn. Reson. Mater. Phys. Biol. Med. 2008; 21(3): 227–235.
28. Vanhamme L, Van Huffel S, Van Hecke P, van Ormondt D. Time-domain quantification of series of biomedical magnetic resonance spectroscopy signals. J. Magn. Reson.. 1999; 140(1): 120–130.
29. Taylor DJ, Styles P, Matthews PM, Arnold DA, Gadian DG, Bore P, Radda GK. Energetics of human muscle: exercise-induced ATP depletion. Magn. Reson. Med. 1986; 3(1): 44–54.
30. Moon RB, Richards JH. Determination of intracellular pH by P-31 magnetic-resonance. J. Biol. Chem.. 1973; 248(20): 7276–7278.
31. Iotti S, Lodi R, Frassineti C, Zaniol P, Barbiroli B. In-vivo assessment of mitochondrial functionality in human gastrocnemius-muscle by P-31 MRS – the role of pH in the evaluation of phosphocreatine and inorganic-phosphate recoveries from exercise. NMR Biomed.. 1993; 6(4): 248–253.
32. Layec G, Bringard A, Le Fur Y, Vilmen C, Micallef JP, Perrey S, Cozzone PJ, Bendahan D. Reproducibility assessment of metabolic variables characterizing muscle energetics in vivo: a P-31-MRS study. Magn. Reson. Med. 2009; 62(4): 840–854.
33. Layec G, Bringard A, Vilmen C, Micallef JP, Le Fur Y, Perrey S, Cozzone PJ, Bendahan D. Does oxidative capacity affect energy cost? An in vivo MR investigation of skeletal muscle energetics. Eur. J. Appl. Physiol. 2009; 106(2): 229–242.
34. Johansen L, Quistorff B. P-31-MRS characterization of sprint and endurance trained athletes. Int. J. Sports Med. 2003; 24(3): 183–189.
35. Layec G, Bringard A, Le Fur Y, Vilmen C, Micallef JP, Perrey S, Cozzone PJ, Bendahan D. Comparative determination of energy production rates and mitochondrial function using different $^{31}$P MRS quantitative methods in sedentary and trained subjects. NMR Biomed.. 2011; 24(4): 425–438.
36. De Feyter HM, van den Broek NMA, Praet SFE, Nicolay K, van Loon LJC, Prompers JJ. Early or advanced stage type 2 diabetes is not accompanied by in vivo skeletal muscle mitochondrial dysfunction. Eur. J. Endocrinol.. 2008; 158(5): 643–653.
37. Arnold DL, Matthews PM, Radda GK. Metabolic recovery after exercise and the assessment of mitochondrial function in vivo in human skeletal muscle by means of P-31 NMR. Magn. Reson. Med. 1984; 1(3): 307–315.
38. van den Broek NMA, De Feyter HMML, de Graaf L, Nicolay K, Prompers JJ. Intersubject differences in the effect of acidosis on phosphocreatine recovery kinetics in muscle after exercise are due to differences in proton efflux rates. Am. J. Physiol. Cell Physiol. 2007; 293(1): C228–C237.
39. Walter G, Vandenborne K, McCully KK, Leigh JS. Noninvasive measurement of phosphocreatine recovery kinetics in single human muscles. Am. J. Physiol. Cell Physiol. 1997; 272(2): C525–C534.
40. Lodi R, Kemp GJ, Iotti S, Radda GK, Barbiroli B. Influence of cytosolic pH on in vivo assessment of human muscle mitochondrial respiration by phosphorus magnetic resonance spectroscopy. Magn. Reson. Mater. Phys. Biol. Med. 1997; 5(2): 165–171. DOI: 10.1007/Bf02592248.
41. Roussel M, Bendahan D, Mattei JP, Le Fur Y, Cozzone PJ. P-31 magnetic resonance spectroscopy study of phosphocreatine recovery kinetics in skeletal muscle: the issue of intersubject variability. Biochim. Biophys. Acta Bioenerg. 2000; 1457(1/2): 18–26.
42. Goudemant JF, Francaux M, Mottet I, Demeure R, Sibomana M, Sturbois X. P-31 NMR saturation transfer study of the creatine kinase reaction in human skeletal muscle at rest and during exercise. Magn. Reson. Med. 1997; 37(5): 744–753.
43. Brehm A, Krssak M, Schmid AI, Nownotny P, Waldhausl W, Roden M. Increased lipid availability impairs insulin stimulated ATP synthesis in human skeletal muscle. Diabetes 2005; 54: A381–A381.
44. Parasoglou P, Xia D, Chang G, Convit A, *Regatte RR*. Three-dimensional mapping of the creatine kinase enzyme reaction rate in muscles of the lower leg. NMR Biomed. 2013. DOI: 10.1002/nbm.2928.
45. Meyerspeer M, Robinson S, Nabuurs CI, Scheenen T, Schoisengeier A, Unger E, Kemp GJ, Moser E. Comparing localized and nonlocalized dynamic $^{31}$P magnetic resonance spectroscopy in exercising muscle


Copyright © 2013 John Wiley & Sons, Ltd.

at 7T. Magn. Reson. Med. 2012; 68(6): 1713–1723. DOI: 10.1002/Mrm.24205.

46. From AHL, Ugurbil K. Standard magnetic resonance-based measurements of the P(i) → ATP rate do not index the rate of oxidative phosphorylation in cardiac and skeletal muscles. Am. J. Physiol. Cell Physiol. 2011; 301(1): C1–C11.
47. Campbellburk SL, Jones KA, Shulman RG. P-31 NMR saturation-transfer measurements in *Saccharomyces cerevisiae* – characterization of phosphate exchange-reactions by iodoacetate and antimycin-a inhibition. Biochemistry 1987; 26(23): 7483–7492.
48. Ugurbil K, Kingsleyhickman PB, Sako EY, Zimmer S, Mohanakrishnan P, Robitaille PML, Thoma WJ, Johnson A, Foker JE, From AHL. P-31 NMR-studies of the kinetics and regulation of oxidative-phosphorylation in the intact myocardium. Ann. NY Acad. Sci. 1987; 508: 265–286.
49. Amara CE, Shankland EG, Jubrias SA, Marcinek DJ, Kushmerick MJ, Conley KE. Mild mitochondrial uncoupling impacts cellular aging in human muscles in vivo. Proc. Natl Acad. Sci. USA 2007; 104(3): 1057–1062.
50. Brindle KM, Radda GK. P-31-NMR saturation transfer measurements of exchange between Pi and ATP in the reactions catalyzed by glyceraldehyde-3-phosphate dehydrogenase and phosphoglycerate kinase in vitro. Biochim. Biophys. Acta 1987; 928(1): 45–55.


Copyright © 2013 John Wiley & Sons, Ltd.